This article has been accepted for publication in IEEE Transactions on Circuits and Systems--II: Express Briefs. This is the author's version which has not been fully edited and content may change prior to final publication. Citation information: DOI 10.1109/TCSII.2023.3252562

Neural Predictor-based Dynamic Surface Parallel Control for MIMO Uncertain Nonlinear Strict-feedback Systems

Yibo Zhang, Wentao Wu, Jinhui Lu, and Weidong Zhang, *Senior Member, IEEE*

***Abstract*—We propose a neural predictor-based dynamic surface parallel control method for a class of uncertain nonlinear systems in this brief. The dynamics of the physical system is in the strict-feedback form and subject to multi-input, multi-output, and uncertain nonlinearities. The parallel control method is developed based on an ACP methodology, including three steps. Firstly, an artificial system to the physical system is developed using an echo state network-based neural predictor structure. Next, a high-order tuner-based computational experiment is developed to achieve online adaptive training of the echo state network. Finally, parallel execution is developed by using a second-order linear tracking differentiator-based dynamic surface control approach. The total closed-loop system can be proved to be input-to-state stable. The effectiveness of the proposed theoretical results is demonstrated by a simulation of trajectory tracking of an autonomous surface vehicle.**

***Index Terms*—Dynamic surface control, parallel control, ACP methodology, strict-feedback systems, neural predictor**

I. Introduction

Tracking control of strict-feedback systems has always been a hot topic [1]–[4]. Many physical systems can be modeled or transformed into strict-feedback systems, such as autonomous marine vehicles, mobile robots, and industrial robots [1]. The backstepping approach is one of the efficient tools for designing tracking controllers for strict-feedback systems [2]–[4]. However, as the order of dynamics increases, backstepping-based controller faces the explosion of complexity due to repeatedly taking the differentiation of virtual control laws. For the purpose of overcoming this issue, the dynamic surface control approach is proposed [5]–[8]. The main feature of the dynamic surface control is adding a first-order filter in every step of the previous backstepping controller design. The derivatives of virtual control laws can be taken by passing through the first-order filter. In order to handle the uncertain nonlinearities in the model, neural dynamic surface control methods are proposed [5], [6]. Subsequently, in [9]–[11], neural predictor-based dynamic surface control approaches are developed by incorporating state predictors into the neural dynamic surface control approach, leading to an improvement in transilient performances. The above dynamic surface controllers in [5]–[11] are only related to states and produced passively. When states change suddenly, the controller will update sharply, leading to a difficult execution [12].

Parallel control theory is proposed to develop controllers for physical systems via an ACP (Artificial systems, Computing experiments, Parallel executions) methodology [12]. The artificial system is an agent model relevant to the physical system. The computational experiment is developed to update and regulate the artificial system. The parallel execution is applied in both the physical and the artificial systems such that the two systems are parallel regulated and controlled. Unlike traditional feedback control, the most feature of parallel control is that the artificial system in the virtual space and the practical system in the physical space are parallel. Several parallel control methods have recently been proposed for linear and nonlinear systems [12]–[15]. However, parallel control of MIMO strict-feedback systems is still open.

Motivated by the above-mentioned observations, we focus on the dynamic surface control of a class of MIMO uncertain nonlinear strict-feedback systems under the framework of parallel control. According to the ACP methodology, the motivation of our design is to divide the control method into an artificial system, a computational experiment, and a parallel execution. Different from the existing parallel control methods [12]–[15] using neural networks directly, the artificial system herein is developed based on the neural predictor. The neural predictor has a better transient performance [16]. In contrast to the existing methods in [5]–[11] under the feedback control framework, the proposed dynamic surface controller is transformed into parallel execution to physical systems. Because of this essential difference, the analysis approaches in [5]–[11] can not be directly applied in this brief. Besides, in contrast to the adaptive identifiers designed in [9]–[11], [17], a high-order tuner is introduced to construct the computational experiment relevant to online adaptive training of the neural network, leading to a higher convergence speed.

Notations Throughout this paper, denote by 0_n an n-dimensional 0-vector. Denote by $\|\cdot\|$ the Euclidean norm of a vector. Denote by $\|\cdot\|_{\mathrm{F}}$ the Frobenius norm of a matrix.

This work was supported in part by the China Post-Doctoral Science Foundation under Grant 2022M722053, in part by the Oceanic Interdisciplinary Program of Shanghai Jiao Tong University under Grant SL2022PT112, in part by the National Natural Science Foundation of China under Grants 52201369 and U2141234, in part by the Hainan Province Science and Technology Special Fund under Grant ZDYF2021GXJS041, and in part by the Shanghai Science and Technology Program under Grants 22015810300 and 19510745200. (*Corresponding Author: Weidong Zhang*)

Yibo Zhang, Wentao Wu and Weidong Zhang are with the Department of Automation, Shanghai Jiao Tong University, Shanghai 200240, China. Weidong Zhang is also with the School of Information and Communication Engineering, Hainan University, Haikou 570228, Hainan, China. Email: {zhang297, wentao-wu, wdzhang}@sjtu.edu.cn. Jinhui Lu is with the Shanghai Ship and Shipping Research Institute Co.,Ltd, Shanghai 200135, China. Email: Lu.jinhui@coscoshipping.com

Denote by $\mathbb{R}^n$ the n-dimensional Euclidean space. Denote by $\mathbb{R}^+$ the positive real space.

II. Preliminary Knowledge

A. Parallel Control

Let us introduce the parallel control briefly. Detailed introductions can refer to [12]–[15]. Consider a physical system $\dot{x} = f(x, u)$, where $x \in \mathbb{R}^m$, $u \in \mathbb{R}^n$, and $f(\cdot) \in \mathbb{R}^m$ denote the state, the control input, and the piecewise continuous function, respectively. In the feedback control framework, u is generated by $u = h(x)$ according to the state information passively. In the framework of the parallel control, an artificial system relevant to the physical system is $\dot{\hat{x}} = \hat{f}(x, \hat{x}, u)$, where $\hat{x}$ is an estimation of x and $\hat{f}(\cdot)$ is an estimation of $f(\cdot)$. u is constructed as a new dynamic system $\dot{u} = h(x, u)$, where $h(\cdot) \in \mathbb{R}^n$ is a piecewise continuous function. The dynamic system executes the physical and artificial systems in parallel according to information interaction.

B. Physical systems

We use a class of MIMO strict-feedback systems to model the physical system considered in this brief as follows

$$\begin{cases} \dot{x}_k = x_{k+1} + f_k(\bar{x}_k), \quad k = 1, ..., n-1 \\ \dot{x}_n = u + f_n(\bar{x}_n) \\ y = x_1 \end{cases} \tag{1}$$

where $x_l \in \mathbb{R}^m$ with $l = 1, ...n$ denotes the system state, $u \in \mathbb{R}^m$ denotes the control input, $y \in \mathbb{R}^m$ is the system output, $\bar{x}_l = [x_1, ..., x_l]^{\mathrm{T}} \in \mathbb{R}^{lm}$ with $l = 1, ...n$ is a state vector, and $f_l(\bar{x}_l) : \mathbb{R}^{lm} \to \mathbb{R}^m$ is an unknown nonlinear function. Define a virtual leader $y_r \in \mathbb{R}^m$. Note that in the real world, many actual physical systems can be modeled by or transformed into an MIMO strict-feedback form, such as autonomous surface vehicles, sensor networks, and industrial robots. Then, we make the following assumption,

Assumption 1. For the physical system (1), (i) $f_l(\bar{x}_l)$ is local Lipschitz in $\bar{x}_l$. (ii) x_l and $\dot{x}_l$ are measurable. (iii) $y_r(t)$ and $\dot{y}_r(t)$ are bounded.

III. Dynamic surface parallel control method design

A. Artificial system design via neural predictor

Step l.($l = 1..., n-1$) At first, recall the l-th order dynamics of the physical system as $\dot{x}_l = x_{l+1} + f_l(\bar{x}_l)$. It can be observed that $f_l(\bar{x}_l)$ is an uncertain nonlinear term. To identify $f_l(\bar{x}_l)$, an echo state network with p reservoir states is utilized [18]

$$f_l(\bar{x}_l) = W_l^{*\mathrm{T}} X_l + \varepsilon_l \tag{2}$$

where $W_l^* \in \mathbb{R}^{p \times m}$ is the output weights matrix, $\varepsilon_l \in \mathbb{R}^m$ is the approximation error with $\|\varepsilon_l\| \leq \varepsilon_l^*$ with $\varepsilon_l^* \in \mathbb{R}^+$, and $X_l \in \mathbb{R}^p$ is the reservoir state vector. The dynamics of X_l is $\dot{X}_l = c_l[-b_l X_l + \sigma(W_{\xi,l}\xi_l + W_{X,l}X_l)]$ where $c_l \in \mathbb{R}^+$ and $b_l \in \mathbb{R}^+$ denote the time coefficient and the decay rate, respectively, $\xi_l = [x_l^{\mathrm{T}}(t), x_l^{\mathrm{T}}(t - t_{\mathrm{d}}), x_{l+1}^{\mathrm{T}}(t)]^{\mathrm{T}} \in \mathbb{R}^{3m}$ denotes the input vector with $t_d \in \mathbb{R}^+$ being a sampling time, $\sigma(\cdot) : \mathbb{R}^{3m} \to \mathbb{R}^m$ denotes the column vector consisting $3m$ Sigmoid-like activation functions, $W_{\xi,l} \in \mathbb{R}^{m \times 3m}$ denotes the sparse connection matrix among reservoir states, $W_{X,l} \in \mathbb{R}^{m \times p}$ denotes the connection matrix among inputs.

Then, the following artificial system associated with the lth-order dynamics of the physical system is designed as

$$\dot{\hat{x}}_l = x_{l+1} + \hat{f}_l - (k_l + \rho_l)(\hat{x}_l - x_l) \tag{3}$$

where $\hat{f}_l = W_l^{\mathrm{T}} X_l$, $k_l \in \mathbb{R}^{m \times m}$ denotes a diagonal control gain, and $\rho_l \in \mathbb{R}^{m \times m}$ is a diagonal parameter matrix.

Step n. recall the nth-order dynamics $\dot{x}_n = u + f_n(\bar{x}_n)$. Letting $x_{n+1} = u + f_n(\bar{x}_n)$, the dynamics of x_{n+1} is

$$\dot{x}_{n+1} = \dot{u} + F(\bar{x}_n) \tag{4}$$

where $F(\bar{x}_n) = \Sigma_{l=1}^{n} \frac{\partial f_n(\bar{x}_n)}{\partial x_l} \dot{x}_l$. Similarly, we can use the following echo state network to recover $F(\bar{x}_n)$

$$F(\bar{x}_n) = W_n^{\mathrm{T}} X_n + \varepsilon_n \tag{5}$$

where the definitions of $W_n^* \in \mathbb{R}^{p \times m}$, $\varepsilon_n \in \mathbb{R}^m$, and $X_n \in \mathbb{R}^p$ are similar to the proceeding step.

An artificial system associated with the $n+1$th-order dynamics of the physical system is designed as follows

$$\dot{\hat{x}}_{n+1} = \dot{u} + \hat{F} - (k_{n+1} + \rho_{n+1})(\hat{x}_{n+1} - x_{n+1}) \tag{6}$$

where $\hat{F} = W_l^{\mathrm{T}} X_l$, $k_{n+1} \in \mathbb{R}^{m \times m}$ denotes a diagonal control gain, and $\rho_{n+1} \in \mathbb{R}^{m \times m}$ is a diagonal parameter matrix.

Then, let x_n pass through a third-order linear tracking differentiator to identify $\dot{x}_{n+1}$ as follows

$$\begin{cases} \dot{\bar{x}}_n = \bar{x}_n^{\mathrm{d}} \\ \dot{\bar{x}}_n^{\mathrm{d}} = \bar{x}_n^{\mathrm{dd}} \\ \dot{\bar{x}}_n^{\mathrm{dd}} = -\mu_a^3[\beta_{n,1}(\bar{x}_n - x_n) + \beta_{n,2}(\frac{\bar{x}_n^{\mathrm{d}}}{\mu_a}) + \beta_{n,3}(\frac{\bar{x}_n^{\mathrm{dd}}}{\mu_a^2})] \end{cases}$$

where $\mu_a \in \mathbb{R}^+$ is the time constant, and $\beta_1, \beta_2, \beta_3 \in \mathbb{R}^+$ are tuning parameters. It has been proved in [19] that there exist $\iota_a^*, \iota_a^{\mathrm{d}*}, \iota_a^{\mathrm{dd}*} \in \mathbb{R}^+$ satisfying $\|\bar{x}_n - x_n\| \leq \iota_a^*$, $\|\bar{x}_n^{\mathrm{d}} - \dot{x}_n\| \leq \iota_a^{\mathrm{d}*}$, and $\|\bar{x}_n^{\mathrm{dd}} - \ddot{x}_n\| \leq \iota_a^{\mathrm{dd}*}$.

Remark 1. The echo state network has a simple structure. Reservoir states are sparsely connected, and the weights are randomly assigned. The input weights are fixed. Besides, the echo state network has fewer tuning parameters. Nevertheless, other types of neural networks can be used as alternatives, such as the single hidden-layer neural network in [9] and the RBF network in [11], [20]. In the approximation property, there is no obvious difference between these different neural networks and the echo state network used in this brief.

B. Computational experiments based on high-order tuners

In the proposed parallel control method, the computational experiment is designed to develop an updating strategy for the echo state network utilized in the artificial system. The update strategy herein is the online adaptation. For the lth-order artificial system with $l = 1, ..., n-1$, a high-order tuner based update law is constructed for W_l^* as follows

$$\begin{cases} \dot{\Theta}_l = -\frac{\gamma_l}{\mathcal{T}_l} X_l e_l^{\mathrm{T}}(\hat{x}_l, x_l) \\ \dot{W}_l = -\Gamma_l(W_l - \Theta_l) \end{cases} \tag{7}$$

This article has been accepted for publication in IEEE Transactions on Circuits and Systems--II: Express Briefs. This is the author's version which has not been fully edited and content may change prior to final publication. Citation information: DOI 10.1109/TCSII.2023.3252562

where $e_l(\hat{x}_l, x_l) = \dot{\tilde{x}}_l + (k_l + \rho_l)\tilde{x}_l$ with $\tilde{x}_l = \hat{x}_l - x_l$, $\mathcal{T}_l = 1 + \|X_l\|^2$, and $\gamma_l \in \mathbb{R}^+$ and $\Gamma_l \in \mathbb{R}^+$ denote two constants. Ref. [21] shows that the high-order tuner enables accelerated learning. The meaning of accelerated learning is to raise the convergence rate of neural networks.

Similarly, for the n+1th-order artificial system, a high-order tuner based update law is constructed for W_l^* as follows

$$\begin{cases} \dot{\Theta}_n = -\frac{\gamma_n}{\mathcal{T}_n} X_n e_n^{\mathrm{T}}(\bar{x}_n^{\mathrm{dd}}, \hat{x}_{n+1}, x_{n+1}) \\ \dot{W}_n = -\Gamma_n(W_n - \Theta_n) \end{cases} \tag{8}$$

where $e_n^{\mathrm{T}}(\bar{x}_n^{\mathrm{dd}}, \hat{x}_{n+1}, x_{n+1}) = \dot{\hat{x}}_{n+1} - \bar{x}_n^{\mathrm{dd}} + (k_{n+1} + \rho_{n+1})\tilde{x}_{n+1}$ with $\tilde{x}_{n+1} = \hat{x}_{n+1} - x_{n+1}$, $\mathcal{T}_n = 1 + \|X_n\|^2$, and $\gamma_n \in \mathbb{R}^+$ and $\Gamma_n \in \mathbb{R}^+$ denote two constants.

C. Parallel execution design based on dynamic surface control

Step 1. Define an error surface for the first-order dynamics of the physical system as $z_1 = y - y_r$, and the dynamics of z_1 satisfies $\dot{z}_1 = x_2 + f_1(\bar{x}_1) - \dot{y}_r$. Then, we can develop the following virtual control law α_1 as follows

$$\alpha_1 = -k_1 z_1 + \dot{y}_r - \hat{f}_1. \tag{9}$$

Without using the first-order filter in the dynamic surface control approaches [5]–[11], a second-order linear tracking differentiator is employed as follows

$$\begin{cases} \dot{v}_1 = v_1^{\mathrm{d}} \\ \dot{v}_1^{\mathrm{d}} = -\mu_1^2[(v_1 - \alpha_1) + 2\frac{v_1^{\mathrm{d}}}{\mu_1}] \end{cases} \tag{10}$$

where $\mu_1 \in \mathbb{R}^+$ denotes a time constant. It has been proved in [19] that there exist $\iota_1^*, \iota_1^{\mathrm{d}*} \in \mathbb{R}^+$ satisfying $\|v_1 - \alpha_1\| \le \iota_1^*$ and $\|v_1^{\mathrm{d}} - \dot{\alpha}_1\| \le \iota_1^{\mathrm{d}*}$. Compared with the first-order filter using in the traditional dynamic surface control design, linear tracking differentiator is capable of disturbance rejection [19].

Step l.($l = 1..., n-1$) Define an error surface for the lth-order dynamics of the physical system as $z_l = x_l - v_{l-1}$, and the dynamics of z_l satisfies $\dot{z}_l = x_{l+1} + f_l(\bar{x}_l) - v_{l-1}^{\mathrm{d}}$. Then, we can develop the following virtual control law α_l as follows

$$\alpha_l = -k_l z_l + v_{l-1}^{\mathrm{d}} - \hat{f}_l - z_{l-1}. \tag{11}$$

An estimated signal v_l related to α_l can be obtained by the following second-order linear tracking differentiator as

$$\begin{cases} \dot{v}_l = v_l^{\mathrm{d}} \\ \dot{v}_l^{\mathrm{d}} = -\mu_l^2\left[(v_l - \alpha_l) + 2\frac{v_l^{\mathrm{d}}}{\mu_l}\right] \end{cases} \tag{12}$$

where $\mu_l \in \mathbb{R}^+$ denotes the time constant. There exist $\iota_l^*, \iota_l^{\mathrm{d}*} \in \mathbb{R}^+$ satisfying $\|v_l - \alpha_l\| \le \iota_l^*$ and $\|v_l^{\mathrm{d}} - \dot{\alpha}_l\| \le \iota_l^{\mathrm{d}*}$.

Step n. Define an error surface for the nth-order dynamics of the physical system as $z_n = x_n - v_{n-1}$, and the dynamics of z_n satisfies $\dot{z}_n = x_{n+1} - v_{n-1}^{\mathrm{d}}$. Then, we can develop the following virtual control law α_n as follows

$$\alpha_n = -k_n z_n + v_{n-1}^{\mathrm{d}} - z_{n-1} \tag{13}$$

where $k_n \in \mathbb{R}^{m\times m}$ denotes a control gain matrix.

Similarly, an estimated signal v_n related to α_n can be obtained by the following tracking differentiator as

$$\begin{cases} \dot{v}_n = v_n^{\mathrm{d}} \\ \dot{v}_n^{\mathrm{d}} = -\mu_n^2[(v_n - \alpha_n) + 2\frac{v_n^{\mathrm{d}}}{\mu_n}] \end{cases} \tag{14}$$

where $\mu_n \in \mathbb{R}^+$ is the time constant. There exist $\iota_n^*, \iota_n^{\mathrm{d}*} \in \mathbb{R}^+$ satisfying $\|v_n - \alpha_n\| \le \iota_n^*$ and $\|v_n^{\mathrm{d}} - \dot{\alpha}_n\| \le \iota_n^{\mathrm{d}*}$.

Step n+1. Define an error surface for the extended state dynamics of the physical systems $z_{n+1} = x_{n+1} - v_n$, and the dynamics of z_n satisfies $\dot{z}_n = \dot{u} + F(\bar{x}_n) - v_n^{\mathrm{d}}$.

A parallel control law u is produced as follows

$$\begin{cases} a_{n+1} = -k_{n+1} z_{n+1} + v_n^{\mathrm{d}} - W_n^T X_n - z_n \\ \dot{u} = u^{\mathrm{d}} \\ \dot{u}^{\mathrm{d}} = -\mu_{n+1}^2\left[(u - \int \alpha_{n+1}\mathrm{d}t) + 2\frac{u^{\mathrm{d}}}{\mu_{n+1}}\right] \end{cases} \tag{15}$$

where $\mu_{n+1} \in \mathbb{R}^+$ denotes the time constant. There exist $\iota_{n+1}^*, \iota_{n+1}^{\mathrm{d}*} \in \mathbb{R}^+$ satisfying $\|u - \int \alpha_{n+1}\mathrm{d}t\| \le \iota_{n+1}^*$ and $\|u^{\mathrm{d}} - \alpha_{n+1}\| \le \iota_{n+1}^{\mathrm{d}*}$. Compared with the feedback control, the proposed parallel control method only adds a differentiator and will not increase the complexity significantly.

IV. Main Results

Theorem 1. Consider the physical system in the MIMO strict-feedback form with the dynamics (1) and the extended n+1th-order dynamics (4). The proposed dynamic surface parallel controller is chosen as the neural predictor-based artificial system (3) and (6), the adaptive computational experiment (7) and (8), and the parallel execution (9), (11), (13), and (15). If *Assumption 1* holds, all subsystems and the total closed-loop system are input-to-state stable.

Proof: The total parallel control closed-loop system is a cascade connection and can be divided into two subsystems. For the artificial system, let $\tilde{x}_l = \hat{x}_l - x_l$, $\tilde{x}_{n+1} = \hat{x}_{n+1} - x_{n+1}$, $\tilde{W}_l = W_l - W_l^*$, $\tilde{W}_n = W_n - W_n^*$, $\tilde{\Theta}_l = \Theta_l - W_l^*$, $\tilde{\Theta}_n = \Theta_n - W_n^*$, and $\iota_a = \bar{x}_n^{\mathrm{dd}} - \dot{x}_{n+1}$, the subsystem consisting of $\tilde{x}_l$, $\tilde{x}_{n+1}$, $\tilde{\Theta}_l$, $\tilde{\Theta}_n$, $\tilde{W}_l$, and $\tilde{W}_n$ becomes as follows

$$\Sigma_{\mathrm{a}}: \begin{cases} \dot{\tilde{x}}_l = -(k_l + \rho_l)\tilde{x}_l - \tilde{W}_l^{\mathrm{T}} X_l - \varepsilon_l \\ \dot{\tilde{x}}_{n+1} = -(k_{n+1} + \rho_{n+1})\tilde{x}_{n+1} - \tilde{W}_n^{\mathrm{T}} X_n - \varepsilon_n \\ \dot{\tilde{\Theta}}_l = -\frac{\gamma_l}{\mathcal{T}_l} X_l(X_l^{\mathrm{T}}\tilde{W}_l + \varepsilon_l^{\mathrm{T}}) \\ \dot{\tilde{W}}_l = -\Gamma_l(W_l - \Theta_l) \\ \dot{\tilde{\Theta}}_n = -\frac{\gamma_n}{\mathcal{T}_n} X_n(X_n^{\mathrm{T}}\tilde{W}_n + \varepsilon_n^{\mathrm{T}} + \iota_a^{\mathrm{T}}) \\ \dot{\tilde{W}}_n = -\Gamma_n(W_n - \Theta_n) \end{cases}$$

where ι_a, ε_l, and ε_n can be regarded as the inputs of the subsystem Σ_{a}. Then, the unforced system $\Sigma_{\mathrm{a},0}$ with respect to the subsystem Σ_{a} is represented by

$$\Sigma_{\mathrm{a},0}: \begin{cases} \dot{\tilde{x}}_l = -(k_l + \rho_l)\tilde{x}_l - \tilde{W}_l^{\mathrm{T}} X_l \\ \dot{\tilde{x}}_{n+1} = -(k_{n+1} + \rho_{n+1})\tilde{x}_{n+1} - \tilde{W}_n^{\mathrm{T}} X_n \\ \dot{\tilde{\Theta}}_k = -\frac{\gamma_k}{\mathcal{T}_k} X_k(X_k^{\mathrm{T}}\tilde{W}_k), \quad k = 1, ..., n \\ \dot{\tilde{W}}_k = -\Gamma_l(\tilde{W}_k - \tilde{\Theta}_k) \end{cases} \tag{16}$$

$\Sigma_{\mathrm{a},0}$ can be proved to be globally exponentially stable at the origin. By applying *Lemma 4.5* in [22], the subsystem Σ_{a} can be proved to be input-to-state stable. Define $\tilde{Z} = [\tilde{z}_1^{\mathrm{T}}, ..., \tilde{z}_{n+1}^{\mathrm{T}}]^{\mathrm{T}}$ with $\tilde{z}_n = 0_3$, $\tilde{\Theta} = [\tilde{\Theta}_1^{\mathrm{T}}, ..., \tilde{\Theta}_n^{\mathrm{T}}]^{\mathrm{T}}$, $\tilde{W} = [\tilde{W}_1^{\mathrm{T}}, ..., \tilde{W}_n^{\mathrm{T}}]^{\mathrm{T}}$, $E_1 = [\|\tilde{Z}\|, \|\tilde{\Theta}\|_{\mathrm{F}}, \|\tilde{W}\|_{\mathrm{F}}]^{\mathrm{T}}$, and $\varepsilon = [\varepsilon_1^{\mathrm{T}}, ..., \varepsilon_n^{\mathrm{T}}]^{\mathrm{T}}$. For all $t > t_0$ and $\tau > t_0$, $E_1(t)$ satisfies

$$\begin{aligned} \|E_1(t)\| \le & \max\{\beta_1(\|E_1(t)\|, t - t_0), \\ & \kappa_\varepsilon(\sup\|\varepsilon(\tau)\|) + \kappa_{\iota_a}(\sup\|\iota_a(\tau)\|)\} \end{aligned}$$

This article has been accepted for publication in IEEE Transactions on Circuits and Systems--II: Express Briefs. This is the author's version which has not been fully edited and content may change prior to final publication. Citation information: DOI 10.1109/TCSII.2023.3252562

where $\beta_1(\cdot)$ is a class $\mathcal{KL}$ function, and $\kappa_\varepsilon(\cdot)$ and $\kappa_{\iota_a}(\cdot)$ are class $\mathcal{K}_\infty$ functions. Merging (9), (11), (13), and (15) into (1) and defining $\iota_k = v_k - \alpha_k$ with $k = 1, ..., n+1$, the subsystem consisting of z_l, z_n, and z_{n+1} becomes as follows

$$\Sigma_{\mathrm{p}}: \begin{cases} \dot{z}_l = -k_l z_l + z_{l+1} - z_{l-1} - \tilde{W}_l^{\mathrm{T}} X_l + \varepsilon_l + \iota_l \\ \dot{z}_n = -k_n z_n + z_{n+1} - z_{n-1} + \iota_n \\ \dot{z}_{n+1} = -k_{n+1} z_{n+1} - z_n - \tilde{W}_n^{\mathrm{T}} X_n + \varepsilon_n + \iota_{n+1} \end{cases}$$

where ι_l, ε_l and $\tilde{W}_l$ can be regarded as the inputs of the subsystem Σ_{p}. Then, the unforced system $\Sigma_{\mathrm{p},0}$ with respect to the subsystem Σ_{p} is given by

$$\Sigma_{\mathrm{p},0}: \begin{cases} \dot{z}_l = -k_l z_l + z_{l+1} - z_{l-1} \\ \dot{z}_n = -k_n z_n + z_{n+1} - z_{n-1} \\ \dot{z}_{n+1} = -k_{n+1} z_{n+1} - z_n. \end{cases} \tag{17}$$

$\Sigma_{\mathrm{p},0}$ can be proved to be globally exponentially stable at the origin. By applying *Lemma 4.5* in [22], the subsystem Σ_{a} can be proved to be input-to-state stable. Define $Z = [z_1^{\mathrm{T}}, ..., z_{n+1}^{\mathrm{T}}]^{\mathrm{T}}$ and $\iota = [\iota_1^{\mathrm{T}}, ..., \iota_{n+1}^{\mathrm{T}}]^{\mathrm{T}}$. For all $t > t_0$ and $\tau > t_0$, $Z(t)$ has

$$\begin{aligned} \|Z(t)\| \leq & \max\{\beta_2(\|Z(t)\|, t - t_0), \varrho_{\tilde{W}}(\sup \|\tilde{W}(\tau)\|_{\mathrm{F}}) \\ & \varrho_\varepsilon(\sup \|\varepsilon(\tau)\|) + \varrho_\iota(\sup \|\iota(\tau)\|)\} \end{aligned}$$

where $\beta_2(\cdot)$ is a class $\mathcal{KL}$ function, and $\varrho_{\tilde{W}}(\cdot)$, $\varrho_\varepsilon(\cdot)$, and $\varrho_\iota(\cdot)$ are class $\mathcal{K}_\infty$ functions. The state $\tilde{W}$ of the subsystem Σ_{a} can be regarded as an input of another subsystem Σ_{p}. By applying *Lemma 4.6* in [22], the total closed-loop system cascaded by Σ_{a} and Σ_{p} can be proved to be input-to-state stable. For all $t > t_0$ and $\tau > t_0$, $Z(t)$ has

$$\begin{aligned} \|Z(t)\| \leq & \max\{\beta_2(\|Z(t)\|, t - t_0), \\ & \varrho_{\tilde{W}} \circ (\kappa_\varepsilon(\sup \|\varepsilon(\tau)\|) + \kappa_{\iota_a}(\sup \|\iota_a(\tau)\|)) \\ & \varrho_\varepsilon(\sup \|\varepsilon(\tau)\|) + \varrho_\iota(\sup \|\iota(\tau)\|)\}. \end{aligned} \tag{18}$$

According to *Definition 4.4* and *Theorem 4.6* in [22], (18) guarantees that for any bounded $\varepsilon(t)$, $\iota(t)$, and $\iota_a(t)$, $Z(t)$ will be bounded. When t increases, $Z(t)$ will be ultimately bounded by class $\mathcal{K}_\infty$ functions of $\sup \|\varepsilon(t)\|$, $\sup \|\iota(t)\|$, and $\sup \|\iota_a(t)\|$. ■

Remark 2. When the system (1) is subject to external disturbances, we can design disturbance observers to observe external disturbances. Besides, when the upper bound of external disturbances is known, we can construct slide mode terms to inhabit the influence of this issue [23]. It is convenient to combine these approaches with the proposed method.

Remark 3. The proposed parallel control method is modular and can extend to other systems on condition that the subsystems are still input-to-state stable. Besides, adaptive approximators and tracking differentiators used herein are alternatives. For example, the RBF network can replace the echo state network, and other command filters can replace the tracking differentiators.

Remark 4. The main challenge in designing the proposed method is how to accurately identify $\dot{x}_{n+1}$ by using the tracking differentiator. The accuracy of $\bar{x}_n^{\mathrm{dd}}$ will influence the performance of the artificial system and the computational experiments.

V. Simulation Example

A simulation example of trajectory tracking of an autonomous surface vehicle is presented in order to show the performance and efficacy of the proposed method. The dynamics of the autonomous surface vehicle is

$$\begin{cases} \dot{\eta} = \nu_{\mathrm{e}} \\ \dot{\nu}_{\mathrm{e}} = u - f(\eta, \nu_{\mathrm{e}}) + w_i \\ f(\eta, \nu_{\mathrm{e}}) = M^{*-1}(C^* \dot{\eta} + D^* \dot{\eta}) \\ R = \begin{bmatrix} \cos\psi & -\sin\psi & 0 \\ \sin\psi & \cos\psi & 0 \\ 0 & 0 & 1 \end{bmatrix} \\ M^* = RMR^{\mathrm{T}},\ C^* = R[C - MR^{\mathrm{T}}\dot{R})]R^{\mathrm{T}},\ D^* = RDR^{\mathrm{T}} \end{cases}$$

where $\eta = [x, y, \psi]^{\mathrm{T}} \in \mathbb{R}^3$, x and y are the latitude coordinate and the longitude coordinate in the earth-fixed coordinate respectively, ψ denotes the yaw angle, $\nu_e = [\bar{u}, \bar{v}, \bar{r}]^{\mathrm{T}} \in \mathbb{R}^3$, $\bar{u}$, $\bar{v}$, $\bar{r}$ represent the surge velocity, sway velocity, and yaw velocity in the earth coordinate respectively, $u = M^{-1*} R\tau \in \mathbb{R}^3$ represents the control input, $M = M^{\mathrm{T}} \in \mathbb{R}^{3\times3}$ is the internal matrix, $R \in \mathbb{R}^{3\times3}$ represents the rotation matrix satisfying $R^{-1} = R^{\mathrm{T}}$, $C \in \mathbb{R}^{3\times3}$ denotes the Coriolis and centripetal matrix, $D \in \mathbb{R}^{3\times3}$ denotes the damping term, and $w \in \mathbb{R}^3$ denotes the external disturbances. Ref. [24] provides internal parameters of matrices defined in the model of the autonomous surface vehicle. The considered trajectory tracking occurs in the part of Beishui Wan, Shanghai, China.

The control parameters are selected as below: $k_1 = \mathrm{diag}\{3, 3, 0.3\}$, $k_2 = \mathrm{diag}\{10, 10, 10\}$, $k_3 = \mathrm{diag}\{10, 10, 10\}$, $\rho_3 = \mathrm{diag}\{20, 20, 20\}$, $\gamma_2 = 50$, $\Gamma_2 = 1000$, $\mu_1 = 7$, $\mu_2 = 70$, $\mu_3 = 70$, and $\mu_a = 70$. The virtual leader is chosen as $y_r = [105\sin(v_s t), 105\cos(v_s t), -v_s t]^{\mathrm{T}}$ with $v_s = 0.009$. The parameters of the echo state network are selected as follows; $t_d = 0.01$, $c_2 = 1$, $b_2 = 1$, $\sigma(s) = (1 - \mathrm{e}^{-s})/(1 + \mathrm{e}^{-s})$, $W_{\xi,2}$ and $W_{X,2}$ are produced randomly, and $W_{X,2}$ is a sparse matrix. Fig. 1 depicts the trajectory of the autonomous surface vehicle, and it can be seen that the autonomous surface vehicle can track along the desired virtual leader. The approximation performance of the echo state network in the artificial system is depicted in Fig. 2. It is shown that the echo state network can approximate uncertain nonlinearities by using the proposed method.

VI. Conclusion

This brief investigates dynamic surface parallel control of physical systems in the MIMO uncertain nonlinear strict-feedback form. For the purpose of dealing with uncertain nonlinearities, an artificial system is constructed based on the echo state network. A high-order tuner-based adaptive computational experiment is designed for the purpose of training the weight of the neural network and raising the

This article has been accepted for publication in IEEE Transactions on Circuits and Systems--II: Express Briefs. This is the author's version which has not been fully edited and content may change prior to final publication. Citation information: DOI 10.1109/TCSII.2023.3252562

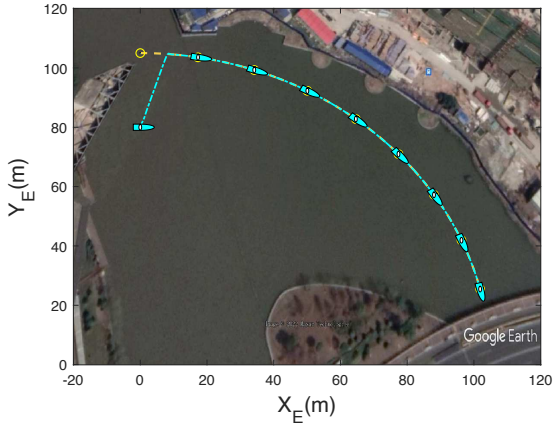

Fig. 1: The trajectory of the autonomous surface vehicle

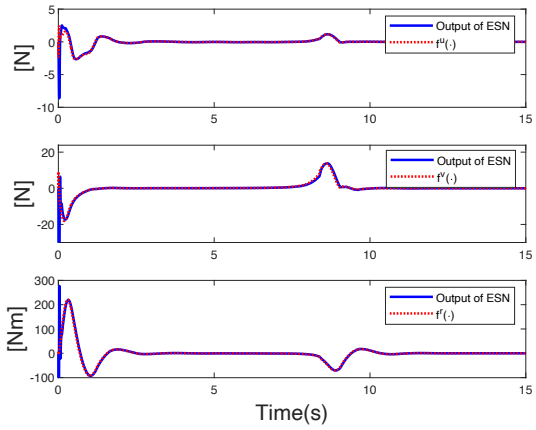

Fig. 2: Approximation performance of the echo state network in the artificial system (ESN: echo state network)

convergence rate. The parallel execution consisting of virtual control laws and a parallel control law is determined by using an improved dynamic surface control method. The theoretical analysis proves the input-to-state stability of the resulting cascaded parallel control closed-loop system. The simulation illustrates the performance of the proposed dynamic surface parallel control method for MIMO uncertain nonlinear strict-feedback systems. In future researches, it is desirable to investigate the output-feedback parallel control problem. Besides, it is rewarding to develop parallel controllers for systems subject to practical constraints.

REFERENCES

[1] S. Gao, Y. Hou, H. Dong, Y. Yue, and S. Li, "Global nested PID control of strict-feedback nonlinear systems with prescribed output and virtual tracking performance," *IEEE Transactions on Circuits and Systems II: Express Briefs*, vol. 67, no. 2, pp. 325–329, 2020.

[2] G. Wen, S. S. Ge, and F. Tu, "Optimized backstepping for tracking control of strict-feedback systems," *IEEE Transactions on Neural Networks and Learning Systems*, vol. 29, no. 8, pp. 3850–3862, 2018.

[3] B. Liu, W. Wang, Y. Li, Y. Yi, and G. Xie, "Adaptive quantized predefined-time backstepping control for nonlinear strict-feedback systems," *IEEE Transactions on Circuits and Systems II: Express Briefs*, vol. 69, no. 9, pp. 3859–3863, 2022.

[4] S. Tong, X. Min, and Y. Li, "Observer-based adaptive fuzzy tracking control for strict-feedback nonlinear systems with unknown control gain functions," *IEEE Transactions on Cybernetics*, vol. 50, no. 9, pp. 3903–3913, 2020.

[5] D. Wang and J. Huang, "Neural network-based adaptive dynamic surface control for a class of uncertain nonlinear systems in strict-feedback form," *IEEE Transactions on Neural Network*, vol. 16, no. 1, pp. 195–202, Jan 2005.

[6] T.-S. Li, D. Wang, G. Feng, and S.-C. Tong, "A DSC approach to robust adaptive NN tracking control for strict-feedback nonlinear systems," *IEEE Transactions on Systems, Man, and Cybernetics, Part B (Cybernetics)*, vol. 40, no. 3, pp. 915–927, 2010.

[7] M. Chen, G. Tao, and B. Jiang, "Dynamic surface control using neural networks for a class of uncertain nonlinear systems with input saturation," *IEEE Transactions on Neural Network Learning System*, vol. 26, no. 9, pp. 2086–2097, Sep 2015.

[8] T. Zhang, M. Xia, and Y. Yi, "Adaptive neural dynamic surface control of strict-feedback nonlinear systems with full state constraints and unmodeled dynamics," *Automatica*, vol. 81, pp. 232–239, 2017.

[9] Z. Peng, D. Wang, and J. Wang, "Predictor-based neural dynamic surface control for uncertain nonlinear systems in strict-feedback form," *IEEE Transactions on Neural Network Learning System*, vol. 28, no. 9, pp. 2156–2167, Sep 2017.

[10] Y. Yang, Q. Liu, D. Yue, and Q.-L. Han, "Predictor-based neural dynamic surface control for bipartite tracking of a class of nonlinear multiagent systems," *IEEE Transactions on Neural Networks and Learning Systems*, vol. 33, no. 4, pp. 1791–1802, 2022.

[11] Y. Yang, Q. Liu, D. Yue, and Y.-C. Tian, "Predictor-based neural dynamic surface control for strict-feedback nonlinear systems with unknown control gains," *IEEE Transactions on Cybernetics*, pp. 1–14, 2021.

[12] Q. Wei, H. Li, and F.-Y. Wang, "Parallel control for continuous-time linear systems: A case study," *IEEE/CAA Journal of Automatica Sinica*, vol. 7, no. 4, pp. 919–928, 2020.

[13] J. Lu, Q. Wei, and F.-Y. Wang, "Parallel control for optimal tracking via adaptive dynamic programming," *IEEE/CAA Journal of Automatica Sinica*, vol. 7, no. 6, pp. 1662–1674, 2020.

[14] Q. Wei, L. Wang, J. Lu, and F.-Y. Wang, "Discrete-time self-learning parallel control," *IEEE Transactions on Systems, Man, and Cybernetics: Systems*, vol. 52, no. 1, pp. 192–204, 2022.

[15] J. Lu, Q. Wei, Y. Liu, T. Zhou, and F.-Y. Wang, "Event-triggered optimal parallel tracking control for discrete-time nonlinear systems," *IEEE Transactions on Systems, Man, and Cybernetics: Systems*, vol. 52, no. 6, pp. 3772–3784, 2022.

[16] Z. Peng, D. Wang, W. Wang, and L. Liu, "Containment control of networked autonomous underwater vehicles: A predictor-based neural dsc design," *ISA transactions*, vol. 59, pp. 160–171, 2015.

[17] Y. Zhang, D. Wang, Z. Peng, and T. Li, "Distributed containment maneuvering of uncertain multiagent systems in MIMO strict-feedback form," *IEEE Transactions on Systems, Man, and Cybernetics: Systems*, vol. 51, no. 2, pp. 1354–1364, 2021.

[18] H. Jaeger, "The "echo state" approach to analysing and training recurrent neural networks-with an erratum note," *Bonn, Germany: German National Research Center for Information Technology GMD Technical Report*, vol. 148, no. 34, p. 13, 2001.

[19] B.-Z. Guo and Z.-L. Zhao, "On convergence of tracking differentiator," *International Journal of Control*, vol. 84, no. 4, pp. 693–701, Apr 2011.

[20] L. Liu, X. Li, Y.-J. Liu, and S. Tong, "Neural network based adaptive event trigger control for a class of electromagnetic suspension systems," *Control Engineering Practice*, vol. 106, p. 104675, 2021.

[21] S. SMcDonald, Y. Cui, J. E. Gaudio, and A. M. Annaswamy, "A high-order tuner for accelerated learning and control," *arXiv preprint arXiv:2103.12868*, 2021.

[22] H. K. Khalil, *Nonlinear Control*. Pearson Education, 2015.

[23] W. Qi, X. Yang, J. H. Park, J. Cao, and J. Cheng, "Fuzzy SMC for quantized nonlinear stochastic switching systems with semi-markovian process and application," *IEEE Transactions on Cybernetics*, vol. 52, no. 9, pp. 9316–9325, 2022.

[24] T. I. Fossen, *Handbook of marine craft hydrodynamics and motion control*. John Wiley & Sons, 2011.